Liquid Crystals
Publication details, including instructions for authors and subscription information:
http://www.informaworld.com/smpp/title~content=t713926090

Dimesogenic compounds consisting of a cholesteryl moiety and an aromatic mesogen interconnected through a central pentamethylene spacer

Soon Wook Cha; Jung-Il Jin; M. Laguerre; M. F. Achard; F. Hardouin

Online publication date: 06 August 2010

To cite this Article Cha, Soon Wook , Jin, Jung-Il , Laguerre, M. , Achard, M. F. and Hardouin, F.(1999) 'Dimesogenic compounds consisting of a cholesteryl moiety and an aromatic mesogen interconnected through a central pentamethylene spacer', Liquid Crystals, 26: 9, 1325 — 1337
To link to this Article: DOI: 10.1080/026782999203995
URL: http://dx.doi.org/10.1080/026782999203995

LIQUID CRYSTALS, 1999, VOL. 26, NO. 9, 1325–1337

Dimesogenic compounds consisting of a cholesteryl moiety and an aromatic mesogen interconnected through a central pentamethylene spacer

SOON WOOK CHA, JUNG-IL JIN
Center for Electro- and Photoresponsive Molecules and Department of Chemistry, Korea University, Seoul 136-701, Korea

M. LAGUERRE
Institut Européen de Chimie et Biologie, Ecole Polytechnique-Universitè Bordeaux I-Universitè Bordeaux II, Avenue Pey Perland-33402 Talence, France

M. F. ACHARD and F. HARDOUIN*
Centre de Recherche Paul Pascal, Université Bordeaux I, Av. A. Schweitzer, 33600 Pessac, France

(*Received 15 January 1999; accepted 1 March 1999*)

New non-symmetric dimesogens consisting of a cholesteryl moiety and an aromatic mesogenic unit interconnected through a pentamethylene spacer have been prepared. The aromatic units consist of two phenyl rings linked by carboxy, oxycarbonyl, ethylene, ethynylene, azo or Schiff's base groups. The mesomorphic and transitional properties have been investigated by using optical microscopy, differential scanning calorimetry, helical pitch measurements, and electric field and miscibility studies. The structures of the mesophases have been studied using X-ray diffraction. Several kinds of smectic packings are observed depending on the nature of the linking group and an attempt to understand the origin of the different phase structures at a molecular level is made.

1. Introduction

Non-symmetric dimesogenic compounds consisting of two structurally different mesogenic groups inter-linked through a central spacer, belong to a new class of liquid crystals that are under intensive studies by several groups [1–25]. From a structural point of view, these systems are interesting since several smectic structures are obtained depending on the molecular parameters. In particular, in the case of the compounds KI-$n(m)$ that contain cholesteryl and Schiff's base moieties linked by an alkylene spacer:

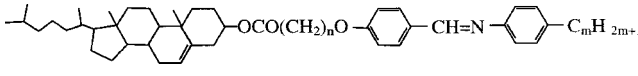

two incommensurate smectic modulations can exist. One corresponds to the length of the cholesteryl part and the other is connected with the overall dimesogen length. Anomalies of periodicity resulting from the competition between these two incommensurate lengths are observed and in some cases the system responds to the frustration connected with this competition by forming either two dimensional modulated smectics or incommensurate smectic phases S_{ic} in which two incommensurate smectic layerings coexist [10, 13, 22, 25].

The complexity of the layered structures is well illustrated by the compound with a pentamethylene spacer ($n = 5$) and a butyl terminal chain ($m = 4$) (KI-5 for short), since its phase sequence involves six different smectics resulting from the condensation of one or the other smectic modulation or from their coexistence in a two-dimensional modulated phase and in an incommensurate fluid smectic phase S_{ic} [10, 22].

Since the richness in the structural aspects of this compound was first observed, we have been studying the influence of molecular variables on the liquid crystalline properties of the homologous compounds [13, 25]. As a part of our continued effort to establish

*Author for correspondence; e-mail: hardouin@crpp.u-bordeaux.fr

Journal of Liquid Crystals ISSN 0267-8292 print/ISSN 1366-5855 online
http://www.tandf.co.uk/JNLS/lct.htm
http://www.taylorandfrancis.com/JNLS/lct.htm

molecular structure–LC property relationships for dimesogenic compounds, this report describes the synthesis and characterization of the following series of compounds:

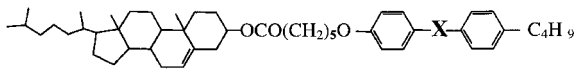

where *X* is –COO– (**6**), –OOC– (**7**), –CH=CH– (**8**) or –C≡C– (**9**). The compounds can be named, respectively, cholesteryl 6-[4-(4-butylphenoxycarbonyl)phenoxy]-hexanoate (compound **6**, KI-5B), cholesteryl 6-[4-(4-butylbenzoyloxy)phenoxy]hexanoate (compound **7** KI-5RB), cholesteryl 6-(4′-butylstilbenyl-4-oxy)hexanoate (compound **8**, KI-5S), cholesteryl 6-(4′-butyltolanyl-4-oxy)-hexanoate (compound **9**, KI5-T). Compounds **6** and **7** have the ester groups in the reverse order and compounds **8** and **9** the vinylene(ethenyl) or the ethynyl group between the benzene rings in the aromatic mesogenic units. Comparisons with the azo compound KI-5A (*X* = –N=N– [22]) and the Schiff's base reference compound KI-5 (*X* = –CH=N– [10, 22]) will be made. The materials corresponding to the general formula (1) are summarized in table 1 together with their acronyms.

2. Experimental

2.1. *Synthesis*

The compounds were synthesized by reacting cholesteryl 6-bromohexanoate (**1**) with 4-butylphenyl 4-hydroxybenzoate, (**2**) 4-hydroxyphenyl 4-butylbenzoate, (**3**) 4-butyl-4′-hydroxystilbene, (**4**) or 4-butyl-4′-hydroxytolane (**5**), in *N*,*N*-dimethylformamide (DMF) in the presence of a base. Since the synthetic procedure was the same for all of the compounds, a representative preparation method is given in detail for compound **6**. This is followed by analytical data for compounds **6**, **7**, **8** and **9**.

Cholesteryl 6-bromohexanoate (1.68 g, 3.0×10^{-3} mol) and 4-butylphenyl 4-hydroxybenzoate (1.00 g, 3.7×10^{-3} mol) were dissolved in 20 ml of DMF containing 0.6 g of K_2CO_3. The mixture was stirred at 120°C for 10 h and then cooled to room temperature. The insoluble material was removed by filtration and the filtrate poured into an excess of water. The precipitate was collected on a filter, and after drying, the crude product was chromatographed through a silica gel column using a mixture of ethyl acetate and *n*-hexane (1 : 5 by volume) as eluent. The yield was 1.80 g (80%), m.p. 102°C.

Table 1. Spacer groups (*X*) and acronyms.

X	Acronym
–COO–	KI-5B
–OOC–	KI-5RB
–CH=CH–	KI-5S
–C≡C–	KI-5T
–N=N–	KI-5A
–CH=N–	KI-5

Compound **6**: ^{1}H NMR spectrum ($CDCl_3$, δ ppm): 0.65 ~ 2.0 (m, 54H, –CH–, $-CH_2-$ and $-CH_3-$), 2.3 (m, 4H, –C=CH–$\underline{CH_2}$ and –OCO–$\underline{CH_2}$–), 2.6 (t, 2H, Ar–$\underline{CH_2}$), 4.0 (t, 2H, –$\underline{CH_2}$–OAr), 4.6 (m, 1H, –O$\underline{CH}$–), 5.38 (m, 1H, –C=$\underline{CH}$–), 6.95 (d, 2H, Ar–$\underline{H}$), 7.10 (d, 2H, Ar–$\underline{H}$), 7.21 (d, 2H, Ar–$\underline{H}$), 8.14 (d, 2H, Ar–$\underline{H}$). IR spectrum (KBr, cm^{-1}): 2926 (aliphatic C–H stretching), 1730 (C=O stretching), 1263 and 1183 (C–O stretching). Anal: calc. for $C_{50}H_{72}O_5$: C 79.74, H 9.64; found C 79.76, H 9.68%.

Compound **7**: ^{1}H NMR spectrum ($CDCl_3$, δ ppm): 0.65 ~ 2.0 (m, 54H, –CH–, $-CH_2-$ and $-CH_3-$), 2.3 (m, 4H, –C=CH–$\underline{CH_2}$– and –OCO–$\underline{CH_2}$–), 2.6 (t, 2H, Ar–$\underline{CH_2}$–), 4,0 (t, 2H, –$\underline{CH_2}$OAr), 4.6 (m, 1H, –O$\underline{CH}$–), 5.38 (m, 1H, –C=CH–), 6.92 (d, 2H, Ar–$\underline{H}$), 7.10 (d, 2H, Ar–$\underline{H}$), 7.30 (d, 2H, Ar–$\underline{H}$), 8.11 (d, 2H, Ar–$\underline{H}$). IR spectrum (KBr, cm^{-1}): 2934 (aliphatic C–H stretching), 1730 (C=O stretching), 1249 and 1169 (C–O stretching). Anal: calc. for $C_{50}H_{72}O_5$: C 79.74, H 9.64; found C 79.64, H 9.68%.

Compound **8**: ^{1}H NMR spectrum ($CDCl_3$, δ ppm): 0.65 ~ 2.0 (m, 54H, –CH–, $-CH_2-$ and $-CH_3-$), 2.3 (m, 4H, –C=CH–$\underline{CH_2}$– and –OCO–$\underline{CH_2}$–), 2.6 (t, 2H, Ar–$\underline{CH_2}$–), 4,0 (t, 2H, –$\underline{CH_2}$OAr), 4.6 (m, 1H, –O$\underline{CH}$–), 5.38 (m, 1H, –C=$\underline{CH}$–), 6.88 (d, 2H, Ar–$\underline{H}$), 7.00 (d, 2H, Ar–$\underline{CH=CH}$–Ar), 7.16 (d, 2H, Ar–$\underline{H}$), 7.42 (d, 2H, 2H, Ar–$\underline{H}$). IR spectrum (KBr, cm^{-1}): 2941 (aliphatic C–H stretching), 1730 (C=O stretching), 1256 and 1169 (C–O stretching). 964 (*trans* –C=$\underline{C-H}$ stretching). Anal: calc. for $C_{51}H_{74}O_3$: C 83.32, H 10.15; found C 83.37, H 10.17%.

Compound **9**: ^{1}H NMR spectrum ($CDCl_3$, δ ppm): 0.65 ~ 2.0 (m, 54H, –CH–, $-CH_2-$ and $-CH_3-$), 2.3 (m, 4H, –C=CH–$\underline{CH_2}$– and –OCO–$\underline{CH_2}$–), 2.6 (t, 2H, Ar–$\underline{CH_2}$–), 4,0 (t, 2H, –$\underline{CH_2}$OAr), 4.6 (m, 1H, –O$\underline{CH}$–), 5.38 (m, 1H, –C=$\underline{CH}$–), 6.85 (d, 2H, Ar–$\underline{H}$), 7.15 (d, 2H, Ar–H), 7.43 (d, 2H, 2H, –Ar–$\underline{H}$). IR spectrum (KBr, cm^{-1}): 2941 (aliphatic C–H stretching), 1730 (C=O stretching), 1256 and 1169 (C–O stretching). Anal: calc. for $C_{51}H_{72}O_3$: C 83.55, H 9.90; found C 83.49, H 9.99%.

2.2. *Experimental techniques*

The IR and ^{1}H NMR spectra of the intermediates and final compounds were recorded on a Bomem MB FTIR spectrophotometer and a Bruker AM300 spectrometer, respectively.

Thermal transitions of the LC compounds under nitrogen atmosphere were studied using a Perkin-Elmer DSC 7 differential scanning calorimeter. The heating and cooling rates in general were kept at 3°C min^{-1}. Indium was employed as a reference material for calibration of temperature and enthalpy. The peak maximum or minimum point was taken as the transition temperature.

Thermodynamic parameters for phase transitions were obtained from the DSC thermograms.

The optical textures of the mesophases formed by the compounds were observed using a polarizing microscope (Leitz Diavert) equipped with a hot stage (FP-82HT) and an automatic controller (Mettler FP-90). When the sample formed a homeotropic texture on a regular slide glass, a rubbed polyimide substrate was used to observe the optical texture.

The phase structures were determined using X-ray diffraction on powder and aligned samples. The X-ray scattering experiments were carried using an 18 kW rotating anode X-ray source (Rigaku-200) with a Ge(1 1 1) crystal as monochromator. The scattered radiation was collected on a two dimensional detector (Imaging Plate system from Mar Research, Hamburg). The samples were placed in an oven, providing a temperature control of 0.1 K.

Pitch measurements were carried out using the Grandjean–Cano method with a prismatic cell in the planar orientation [26, 27]. Electro-optical properties were studied using commercial cells (from E.H.C., Japan) with rubbed polyimide alignment layers resulting in homogeneously aligned samples. The switching current was obtained by applying a triangular voltage wave using a function synthesizer (Tabor Electronics 8550) and a high power amplifier (Krohn-Hite). Computational methods used for molecular dynamics calculations and to determine electrostatic potential maps have been recently described [25].

3. Results and discussion

3.1. *General comments on phase characterization*†

Up to now, eight different smectic mesophases which have no in-plane order according to X-ray measurements, such as in conventional S_A or S_C phases, have been detected in these dimesogens composed of a cholesteryl mesogenic unit and a classical two aromatic rings mesogenic unit. Since the textures are fairly often comparable, we use a phase nomenclature which corresponds to a structural classification based on the smectic periodicity rather than the tilted or non-tilted nature of the phase (S_C or S_A). Indeed, the smectic layering corresponds either to a periodicity $2\pi/q1$ (where $q1$ is the wave vector) close to the dimesogen length labelled 'S_{q1} phase' or to a layer spacing $2\pi/q3$ (where $q3$ is the wave vector) smaller than half the molecular length labelled 'S_{q3} phase'. By reference to polar smectics, these smectic periodicities are analogous to a bilayer smectic A_2 and to a monolayer smectic A_1, respectively. Frustration resulting from the competition between these two incommensurate lengths gives rise to two dimensional modulated smectics ($S_{\tilde{C}}$ ribbon phase [28] or $S_{\tilde{A}}$ antiphase [29]) or to incommensurate fluid smectic phases S_{ic} [10, 22, 25]. As illustrated by the complex phase sequence of the reference compound KI-5 shown below, this nomenclature centred on structural differences remains insufficient to distinguish between phases with similar smectic layering (e.g. 'S_{q1}' phases). Nevertheless, this phase assignment will not be improved upon until results of additional experiments, such as misciblity studies with different smectic phases, electric field effect studies etc are known in detail.

$$Cr \rightarrow S_{\tilde{C}} \rightarrow S_{q3} \rightarrow S_{ic} \rightarrow S_{q1LT} \rightarrow S_{q1HT} \rightarrow TGB_{q1} \rightarrow N^* \rightarrow I$$

As depicted in figure 1, the nature of the smectic packing depends on the relative lengths of the spacer n and the terminal chain m in the KI-$n(m)$ series. The role of these two parts appears basically different [13, 25] since a lengthening of the spacer leads to the disappearance of the '$q1$' periodicity [figure 1 (*a*)] while on the contrary, long terminal chains favour this type of smectic layering [figure 1 (*b*)]. In this report, we keep n and m constant ($n = 5$, $m = 4$) in order to investigate the influence of the linking group X on the smectic arrangement.

3.2. *Phase characterization of the KI-5X compounds*

The thermal transitional behaviour of the compounds was examined by DSC and an initial characterization of the liquid crystalline phases was made using polarizing optical microscopy. X-ray diffraction experiments were performed to obtain structural identification, and results are summarised in table 2.

3.2.1. *Mesomorphic properties*

Figures 2 (*a–e*) show the DSC thermograms of the compounds KI-5X. In addition to the melting peak corresponding to a large enthalpy change (25–45 kJ mol^{-1}), the materials show reversible thermal transitions indicating enantiotropic mesophases. Only KI-5RB does not crystallize readily when the LC phase is cooled, but when heated again, it undergoes a crystallization and a melting process.

On cooling from the isotropic liquid, all the members of the KI-5X series exhibit cholesteric mesophases with characteristic Grandjean textures (figure 3). As illustrated in figure 4, changing the linking group from X = –CH=CH– to –CH=N–, –N=N, –C≡C–, –COO– and –OOC– causes the clearing temperature to decrease indicating that the mesomorphic order is progressively destabilized. Except in the case of the last compound with the –OOC– linking group (KI-5RB), the cholesteric phase is followed by additional smectic mesophases.

† In view of the complexity of the phase sequences and phase types exhibited by their new dimesogens, and the as yet incomplete nature of their study, the old nomenclature system using S rather than Sm to represent a smectic phase has been retained in this paper (Ed).

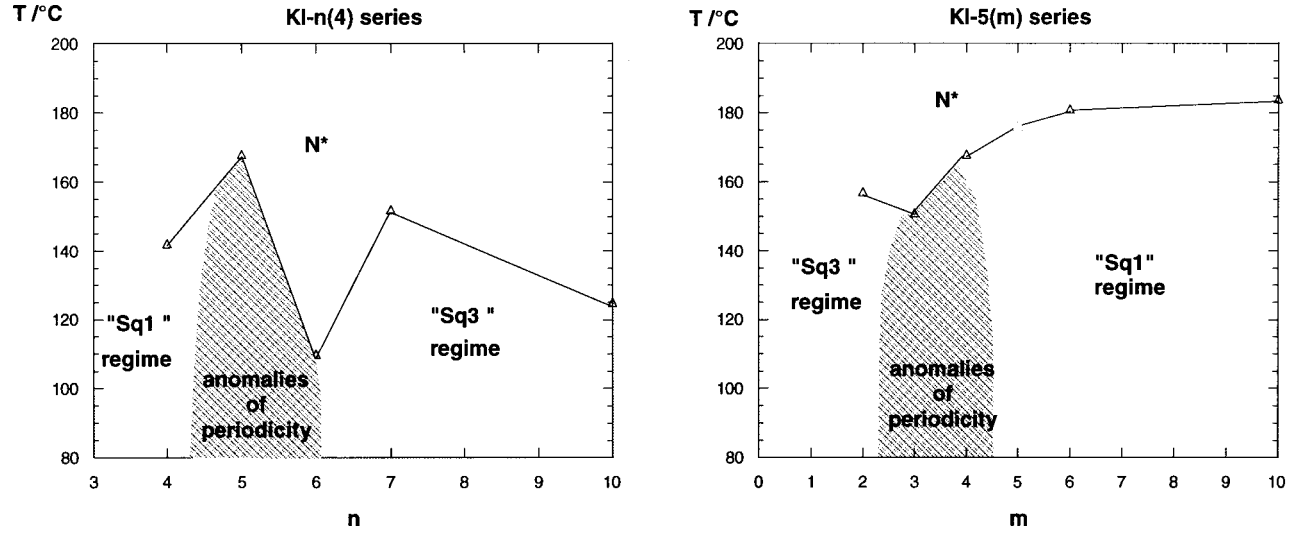

Figure 1. Evolution of the smectic packing in the KI-$n(m)$ series with (*a*) spacer length n and (*b*) terminal chain length m: 'S_{q1}' regime corresponds to bilayer smectic phases in which the layer thickness is close to the dimesogen length, 'S_{q3}' regime corresponds to monolayer smectic phases with a layer thickness imposed by the cholestryl moiety. For specific molecular parameters, a frustration appears which generates 'anomalies of periodicity', e.g. smectic phases with unusual density modulation, modulated two dimensional smectics or incommensurate fluid smectics.

Table 2. Transition temperatures (°C) and enthalpies in brackets (kJ mol^{-1}). Cr = crystalline phase, S = smectic phase (for the different indices used, see the text), TGB = twist grain boundary, N* = cholesteric, I = isotropic liquid.

Compound	X	Phase transition temperatures (°C) and enthalpies (kJ mol^{-1})
KI-5S	–CH=CH–	$Cr \xrightarrow[(29.2)]{125\,^{\circ}C} S_{q3} \xrightarrow{190\,^{\circ}C} TGB_{q3}\ (S\text{–}TGB\text{–}N^{*}: 3.08) \xrightarrow{191.7\,^{\circ}C} N^{*} \xrightarrow[(3.7)]{206.5\,^{\circ}C} I$
KI-5	–CH=N–	$Cr \xrightarrow{85\,^{\circ}C} S_{C} \xrightarrow{97\,^{\circ}C} S_{q3} \xrightarrow{141\,^{\circ}C} S_{ic} \xrightarrow{146\,^{\circ}C} S_{q1LT} \xrightarrow{152\,^{\circ}C} S_{q1HT} \xrightarrow{165\,^{\circ}C} TGB_{q1} \xrightarrow{168\,^{\circ}C} N^{*} \xrightarrow{192\,^{\circ}C} I$
KI-5A	–N=N–	$Cr \xrightarrow[(25.3)]{113\,^{\circ}C} S_{A} \xrightarrow[(0.17)]{137\,^{\circ}C} S_{q1} \xrightarrow{160\,^{\circ}C} TGB_{q1}\ (S\text{–}TGB\text{–}N^{*}: 0.92) \xrightarrow{163\,^{\circ}C} N^{*} \xrightarrow[(3.4)]{194\,^{\circ}C} I$
KI-5T	–C≡C–	$Cr_1 \xrightarrow[(Cr^1\text{–}Cr^2\text{–}S: 26.3)]{93\,^{\circ}C} Cr_2 \xrightarrow{99\,^{\circ}C} S_{q1} \xrightarrow{146\,^{\circ}C} TGB_{q1}\ (S\text{–}TGB\text{–}N^{*}: 0.37) \xrightarrow{150.5\,^{\circ}C} N^{*} \xrightarrow[(3.4)]{185.4\,^{\circ}C} I$
KI-5B	–COO–	$Cr \xrightarrow[(44.9)]{119\,^{\circ}C} S_{q1} \xrightarrow{142\,^{\circ}C} TGB_{q1}\ (S\text{–}TGB\text{–}N^{*}: 0.3) \xrightarrow{144\,^{\circ}C} N^{*} \xrightarrow[(3.3)]{180.8\,^{\circ}C} I$
KI-5RB	–OOC–	$Cr \xrightarrow[(30.8)]{85\,^{\circ}C} N^{*} \xrightarrow[(2.9)]{175.5\,^{\circ}C} I$

With the same sequence of X, the cholesteric–smectic transition temperature decreases, showing that the layered structures are progressively disfavoured (figure 4 and table 2).

Interestingly enough, KI-5B forms smectic and cholesteric mesophases, whereas KI-5RB shows only a cholesteric phase. The only difference between the two compounds lies in the structure of linking group –COO–

Figure 2. DSC thermograms of the KI-5X series on heating and cooling at 3°C min^{-1}: (*a*) KI-5S (X = –CH=CH–), (*b*) KI-5 reference compound (X = –CH=N–), (*c*) KI-5A (X = –N=N–), (*d*) KI-5T (X = –C≡C–), (*e*) KI-5B (X = –COO–), (*f*) KI-5 RB (X = –OCO–). Enlarged details are shown in the insets. The published thermogram of the reference compound KI-5 is recalled for comparison.

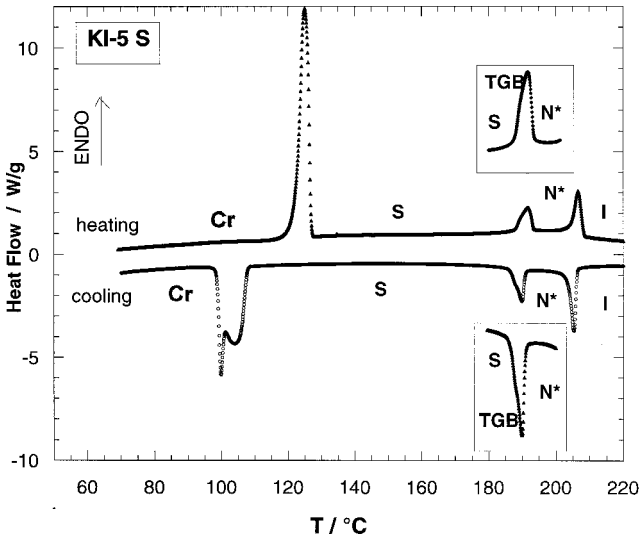

(*a*)

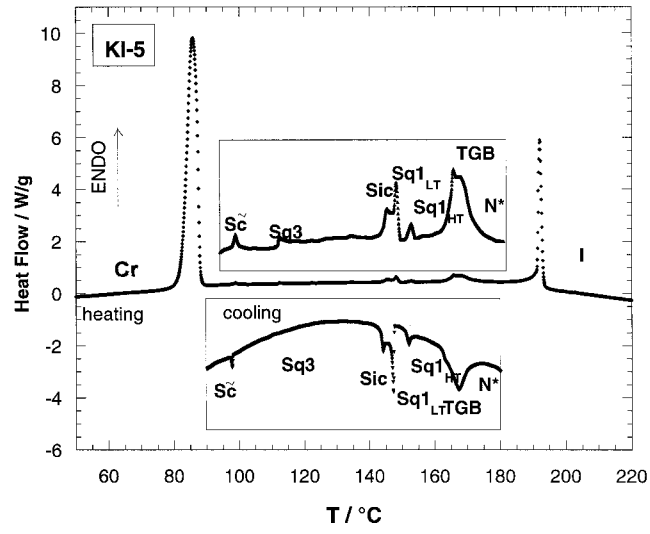

(*b*)

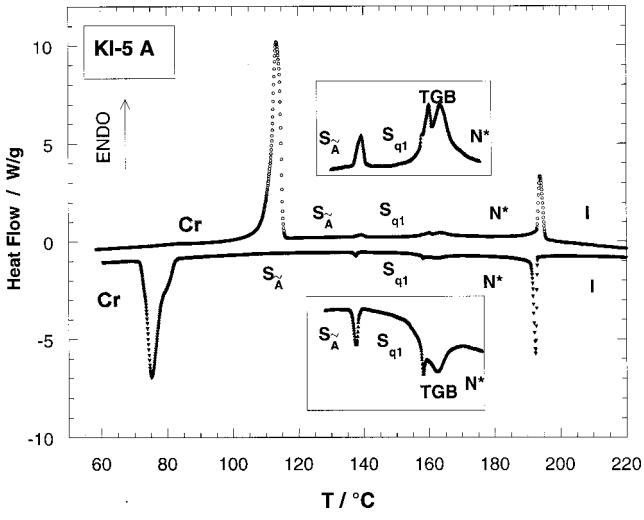

(*c*)

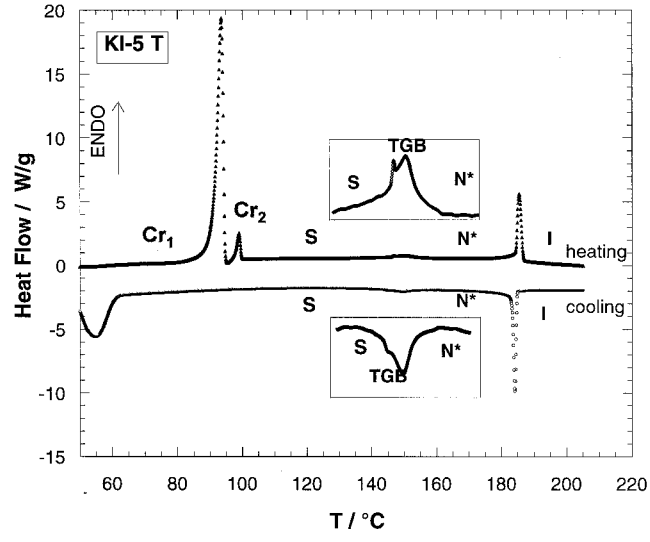

(*d*)

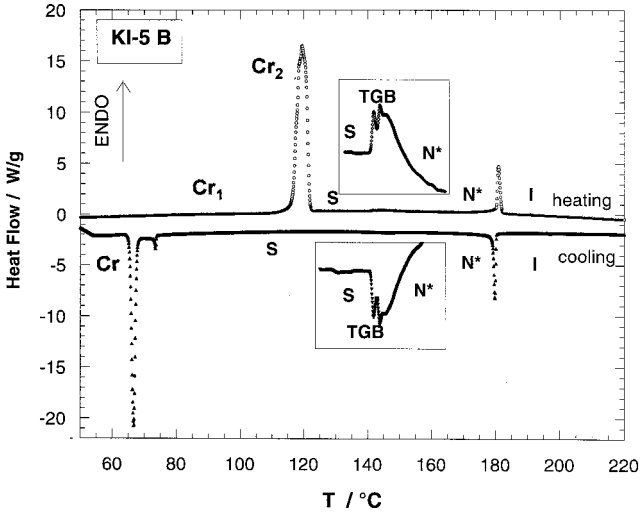

(*e*)

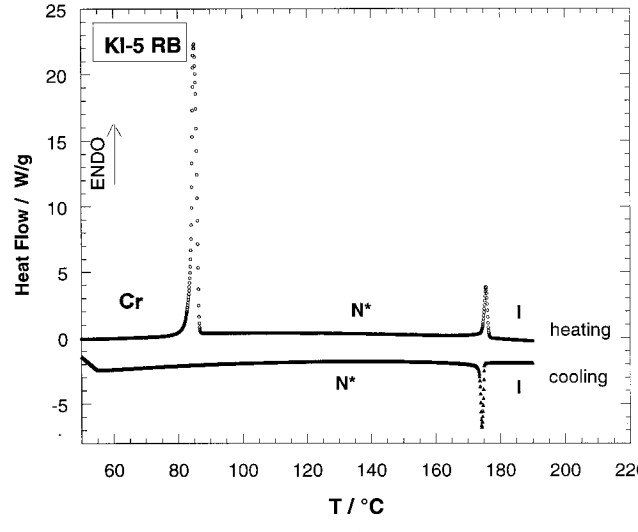

(*f*)

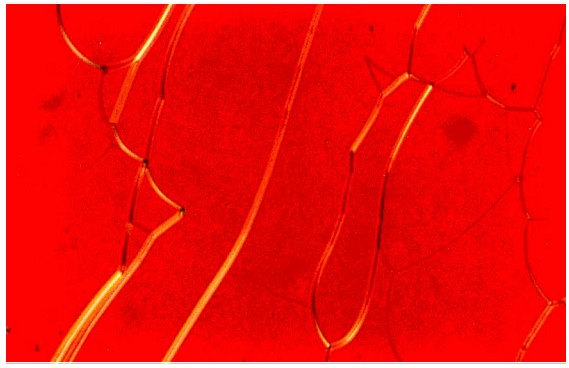

Figure 3. Grandjean texture of the cholesteric phase of KI-5S at 192°C.

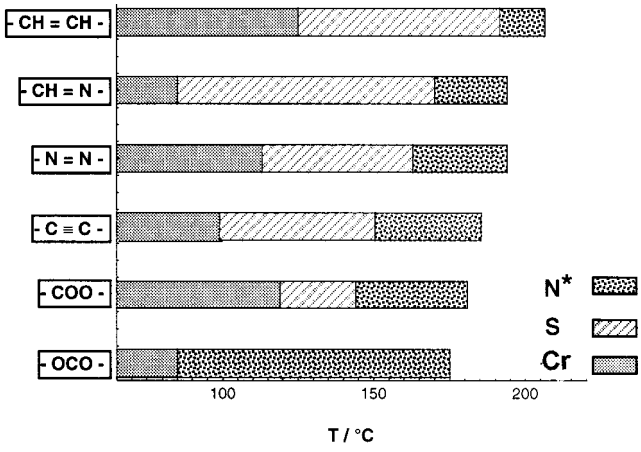

Figure 4. Schematic representation of the mesomorphic ranges for the KI-5*X* compounds.

vs. –OOC–. In fact, a similar observation has been made for some conventional two aromatic ring LC materials for which the –OOC– linking groups destabilizes the smectic phase [30]:

$C_8H_{17}O–C_6H_4–COO–C_6H_4–C_9H_{19}$

Cr 53 SmA 66 N 69 I (°C)

$C_8H_{17}O–C_6H_4–OOC–C_6H_4–C_9H_{19}$

Cr 53 [SmA 48] N 63 I (°C)

As shown in table 2, by comparison with the KI-5 reference compound, simpler phase sequences are observed for the KI-5*X* homologous under study. Cooling from the cholesteric phase, the first smectic encountered is a TGB phase. As for KI-5, the assignment of TGB phase was made from the observation of the characteristic vermis (figure 5) and planar Grandjean textures and by the existence of a resolution-limited X-ray peak at low angles. Note that the TGB phase is the same for KI-5, KI-5A, KI-5T, and KI-5B. For these

Figure 5. Vermis texture of the TGB phase of KI-5T at 145°C (no surface treatment).

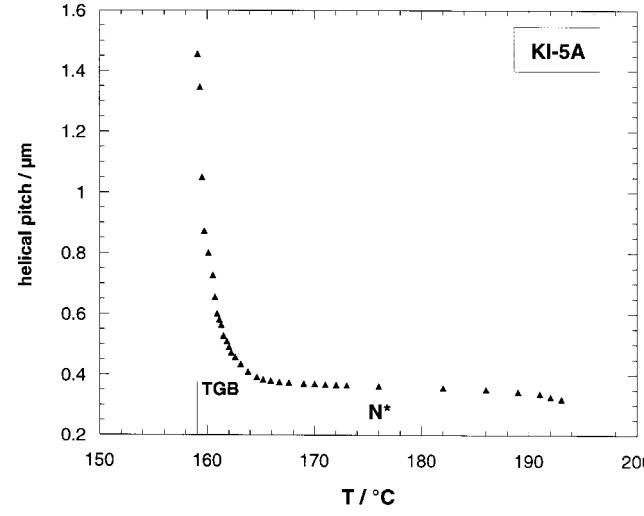

Figure 6. Thermal evolution of the helical pitch in the cholesteric and TGB phases of the compound KI-5A.

Figure 7. Columnar texture of the TGB phase of KI-5S at 187°C.

compounds, the cholesteric pitch length increases considerably at the N*–TGB transition and becomes too long for reflection to occur in the visible range. Figure 6 shows as an example the thermal evolution of the helical pitch for KI-5A.

In the case of KI5-S (–CH=CH–), the pitch regularly increases with decreasing temperature in the cholesteric phase (0.55 μm at 205°C and 0.75 μm at 192°C) and no divergence occurs at the N*–TGB transition. This corroborates the microscopic observations which suggest another kind of TGB phase with columnar textures (figure 7) instead of a Grandjean texture. Columnar textures have been reported for the TGBA phase of a conventional rod-like mesogen [31] and for the TGB_{q3} phase of long spacers dimesogens KI-7(4) and KI-10(4) [13].

With no surface treatment a homeotropic texture spontaneously develops for the smectic phases of the KI-5*X* compounds which appear like uniaxial media where the molecules are on average parallel or symmetrically disposed with respect to the viewing direction. With a rubbed polyimide substrate, fan-shaped textures are observed with several textural variants which can occur in the same preparation depending on the thermal history of the sample (slow or fast heating or cooling) and on the alignment process. Some examples are given in figure 8 and it is clearly evident that these textural variants prevent any unquestionable identification. Nevertheless, microscopic observations confirm that the smectic phases of the KI-5*X* compounds can be switched on applying a strong electric field.

3.2.2. *Structural properties*

Intensity profiles corresponding to the X-ray patterns of the smectic phases of the KI-5*X* compounds are shown in figure 9.

For all the KI-5*X* compounds, the diffuse scattering in the wide angle region (see insets) gives evidence that there is no long range positional order within the layers. Thus the smectic phases are low ordered smectics (i.e. 'fluid smectics'). In the small angle region, the characteristic features of the X-ray patterns are not identical for all the KI-5*X* dimesogens.

Two equally spaced Bragg reflections $q1 = 0.151$ Å^{-1} and $2q1$ (1st and 2nd order) are observed for KI-5T. The layer thickness $d = 2\pi/0.151$ Å^{-1} $= 41.6$ Å is not temperature dependent. The smectic phase of KI-5T corresponds to a 'S_{q1} phase' as observed at high temperature for KI-5A ($q1 = 0.156$ Å^{-1} $d = 2\pi/0.156$ Å^{-1} $=$ 40.2 Å) and for the $S_{q1\,LT}$ phase of KI-5 ($q1 = 0.151$ Å^{-1} $d = 2\pi/0.151$ Å^{-1} $= 41.6$ Å). For KI5-T the layer spacing is shorter than the molecular length measured in the most extended conformation (44.3 Å) and this suggests that the dimesogens which are forming the layered structure are bent and/or tilted with respect to the layer normal.

The smectic phase of KI-5B is characterized by a wave vector $q1 = 0.147$ Å^{-1} at 140°C with a very weak harmonic. It corresponds to a 'S_{q1} phase'. The layer spacing d slightly increases with decreasing temperature ($d = 2\pi/0.147$ Å^{-1} $= 43$ Å at 140°C to $d = 2\pi/0.142$ Å^{-1} $=$ 44.2 Å at 95°C) but remains shorter than the molecular length.

The patterns of the smectic phase of KI-5S are characterized by one resolution limited peak at $q3 = 0.313$ Å^{-1}. According to our nomenclature this phase is labelled 'S_{q3} phase'. The layer spacing $d = 20.0$ Å is not temperature dependent and corresponds to the length of the cholesteryl moiety as already observed for the KI-*n*(*m*) series [10, 13, 22, 25]. With decreasing temperature, a diffuse peak centred at an incommensurate wavenumber $q1 = 0.175$ Å^{-1} with respect to the wavevector $q3$ is observed. It probably corresponds to two dimensional smectic fluctuations, suggesting a possible modulated smectic like that for KI-5A or KI-5. Nevertheless, since up to now we could not obtain a perfectly oriented sample of this phase, a structural model cannot be proposed. Finally, one can note that crystallization occurs through a layered structure with a wave vector $q = 0.111$ Å^{-1} and two harmonics.

The last compound with a –OOC– linking group (KI-5RB) does not show a Bragg peak in the small angle region, confirming its cholesteric morphology. Nevertheless, two diffuse peaks at $q = 0.194$ Å^{-1} $= 2\pi/32.4$ Å and 0.330 Å^{-1} $= 2\pi/18.8$ Å suggest, despite the cholesteric state, the existence of two incommensurate smectic modulations.

To summarize (table 3), KI-5S shows a 'S_{q3} phase' with a layer parameter less than half the molecular length, connected with the length of the cholesterol moiety, while the smectic phases of KI-5T, KI-5A, KI-5B, labelled as 'S_{q1} phases', are characterized by a layer spacing close to, but shorter than the dimesogen length. Additional experiments are needed for further identification.

3.2.3. *Additional experiments: electric field effects and miscibility studies*

As shown on the photomicrographs of figure 8, the smectic phases of the KI-5*X* homologues orient on applying a sufficiently high electric field. Figure 10 shows the electrical response of a 4 μm thick cell with a planar

Table 3. Layer spacing d for the KI-5*X* homologues. Comparison with the molecular length L in an all *trans*-conformation.

Compound	*X*	*d*/Å	*d*/*L*	phase
KI-5S	–C=C–	20.0 (150°C)	0.45	S_{q3}
KI-5	–CH=N–	41.6 (150°C)	0.93	S_{q1}
KI-5A	–N=N–	40.2 (150°C)	0.91	S_{q1}
KI-5T	–C≡C–	41.6 (140°C)	0.93	S_{q1}
KI-5B	–COO–	43.0 (140°C)	0.97	S_{q1}

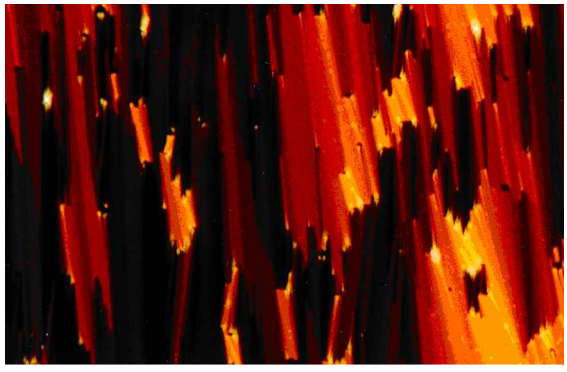

(*a*)

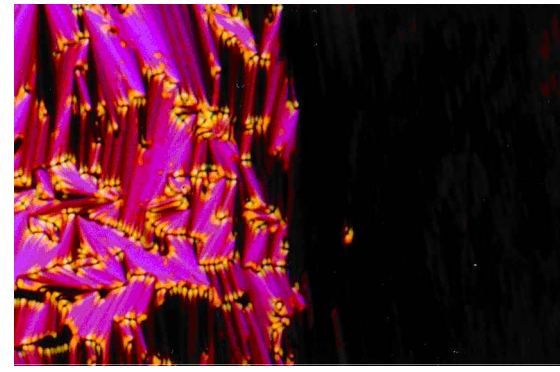

(*b*)

(*c*)

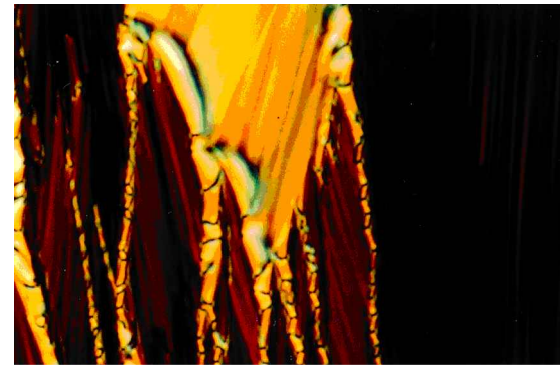

(*d*)

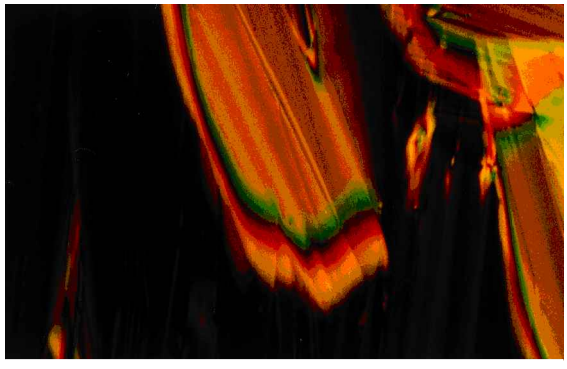

(*e*)

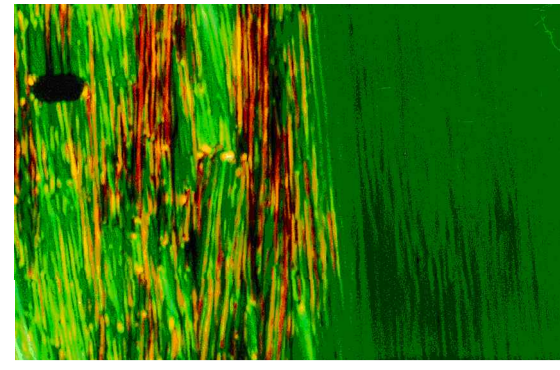

(*f*)

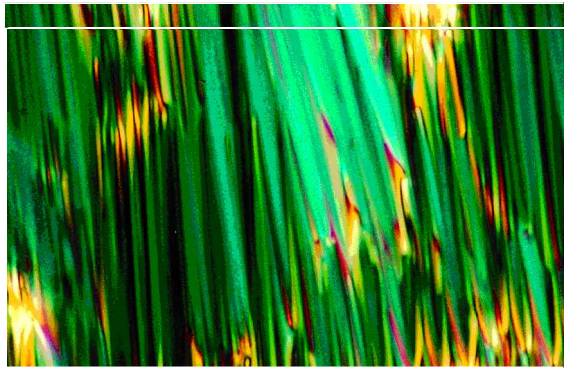

(*g*)

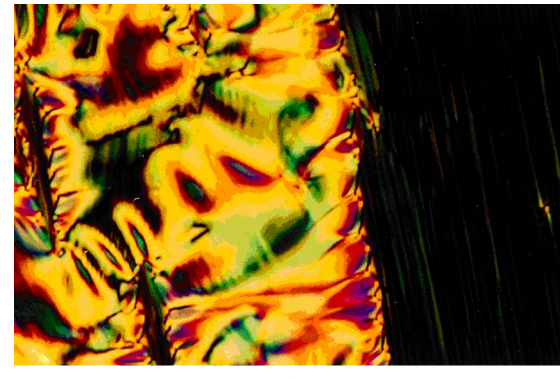

(*h*)

alignment layer, under a triangular wave voltage in the case of KI-5S in the S_{q3} phase at 170°C. The frequency was 20 Hz, the amplitude $\pm$ 80 V. The threshold voltage is high (65 V). Two current peaks are recorded during a half period suggesting a kind of antiferroelectric behaviour. Nevertheless, one can notice that the current peaks are broad and the polarization is not zero at zero field, which must be the case for antiferroelectric S^*_{CA}. In addition the same electric response is observed for the S_{q1} phases of KI-5T, KI-5B and KI-5A. From these first observations, the study of the electric field effects appears much more difficult compared with that for ordinary calamitic compounds and at this time does not help us to differentiate the smectic phases of the KI-5*X* compounds under study.

From miscibility studies we first note that the KI-5/KI-5A binary diagram, obtained from mixtures of KI-5A with the reference compound KI-5, allows the 'S_{q1} phase' of KI-5A to be identified with the $S_{q1_{LT}}$ phase of KI-5 [22] [schematic drawing, figure 11 (*a*)]. Since phase diagrams constructed by preparing mixtures with definite concentrations are very time consuming to establish, we used in this study the contact method‡ to compare the smectic phases of the KI-5*X* homologues with the S_{q1} phase of KI-5A.

A contact diagram [figure 11 (*b*)] between KI-5A and KI-5T demonstrates the complete miscibility between the S_{q1} and the TGB_{q1} phases of the two compounds. The same diagram is obtained for the KI-5A/KI-5B system.

In contrast, the KI-5A/KI-5S diagram [figure 11 (*c*)] exhibits a non ideal behaviour accompanied by a clear distinction between S_{q1} and S_{q3} phases and the TGB_{q1} and TGB_{q3} phases.

To summarize, miscibility studies identify the S_{q1} phase of KI-5A, KI-5T and KI-5B with the $S_{q1_{LT}}$ phase of the KI-5 reference compound, and show that the TGB_{q1} phases of these four compounds are the same. On the other hand, the S_{q3} phase of KI-5S is different from the S_{q1} phases and from an antiphase ($S_{\tilde{A}}$) despite the two dimensional tendency revealed by the 2D-fluctuations observed by X-ray analysis.

‡ A small quantity of each component is melted on opposite sides of a cover slip on a slide and allowed to flow to come in contact: a diffusion of one into the other occurs. The domain of mixing exhibits all the molar fractions for the binary system and microscopic investigation of this part provides the thermodynamic characteristics of the phase diagram (but not of course the concentrations).

3.3. *Discussion*

The only difference between the KI-5*X* compounds lies in the nature of the linking group *X* between the two aromatic rings. Nevertheless, despite their similar chemical formulae and comparable molecular lengths, the molecules of these compounds give rise to different smectic packings. Distinct layered structures may result from subtle variations of the local arrangement of the dimesogens. Indeed, we have recently shown by molecular mechanics calculations that a lower energy configuration of two adjacent dimesogens corresponds to an antiparallel association, and that their overlapping is a result of the balance between the electrostatic and the van der Waals interactions [25]. A small modification of the chemical structure will modify the equilibrium between these two types of interaction and, as a consequence, the pair conformation and thus the smectic layering order. Note that for dimesogens composed of the cholesteryl moiety linked to an aromatic mesogen through an alkyl spacer, the negative potentials are strongly localized along the molecule and centred on the COO group of the cholesteryl part and on the oxygen and the linking group of the aromatic mesogen.

Our earlier studies on the KI-5(*m*) series, depending on the length of the aliphatic parts, showed that for short aliphatic tails, the overlapping obtained for antiparallel pairing corresponds to a regular alternation of the negative and positive potentials. The smectic order connected to $q3$ experimentally observed may result from these favourable interactions between the two kinds of mesogenic groups: the cholesteryl moiety can then impose a characteristic length relative to $q3$, since the aromatic mesogenic part is able to adapt to its layering size. In the case of long aliphatic tails, this perfect matching of the negative and positive parts is no longer present, particularly in the spacer region, and unfavourable interactions between negative lobes are observed. This unfavourable repartition of the electrostatic potential around half the length of the dimer may account for the loss of the characteristic length connected with $q3$ and for the development of a periodicity connected to $q1$.

Figure 8. Texture variants of the smectic phases of KI-5*X* compounds on rubbed polyimide substrates resulting in random planar alignment of the molecules. The application of an electric field aligns the samples. KI-5S at 155°C: (*a*) texture reminiscent of a relatively poor alignment of an antiferroelectric S^*_C (*b*) '$S_{\tilde{A}}$' fan-shaped texture (left) and texture resulting on the application of an electric field (right). KI5-T at 140°C: (*c*) untypical S_C texture with two alignment directions, (*d*) focal-conic texture (left) and texture resulting on the application of an electric field (right). KI-5A at 150°C: (*e*) focal-conic textures with two types of alignment domains, (*f*) fan-shaped texture (left) and texture resulting on the application of an electric field (right). KI-5B at 139°C: (*g*) focal-conic texture, (*h*) untypical texture (left) and texture resulting on the application of an electric field (right).

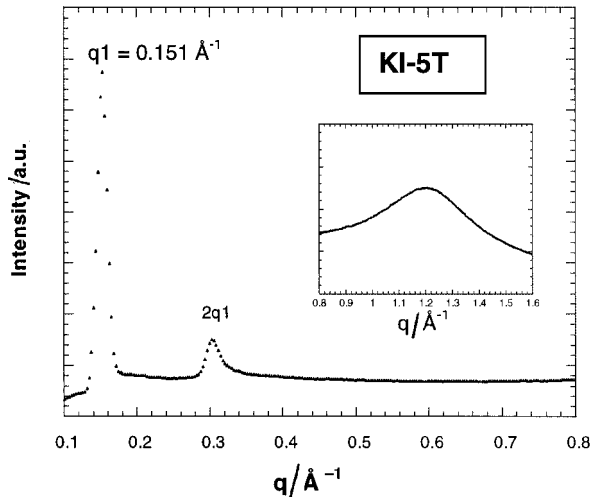

(*a*)

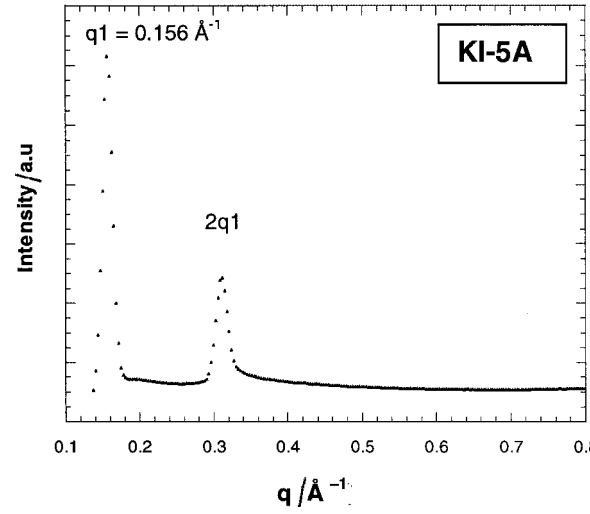

(*b*)

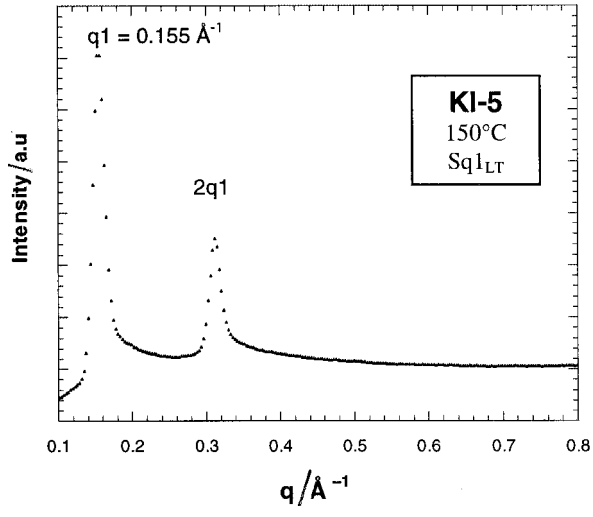

(*c*)

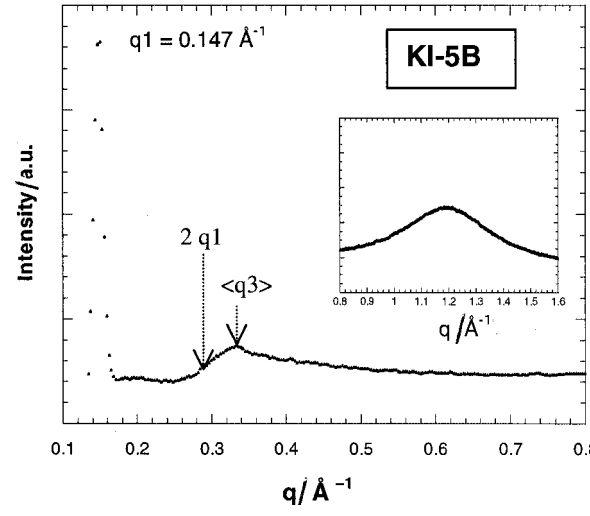

(*d*)

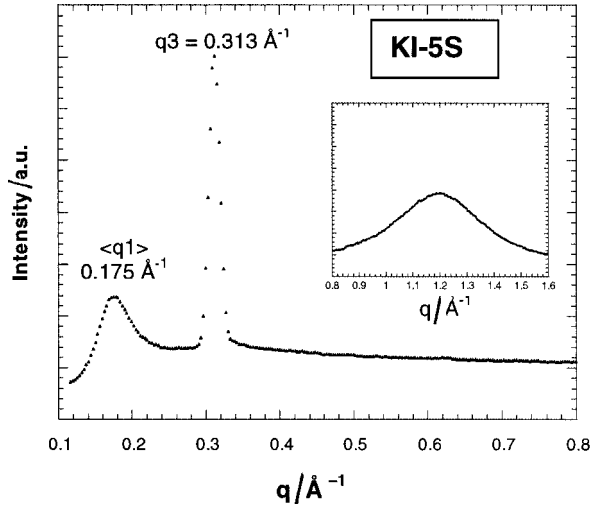

(*e*)

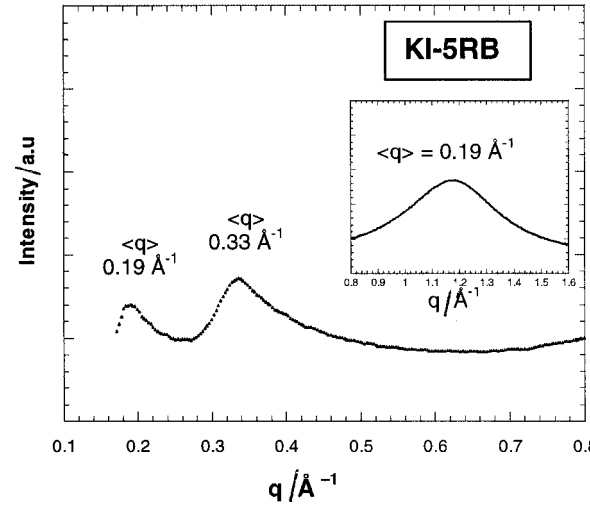

(*f*)

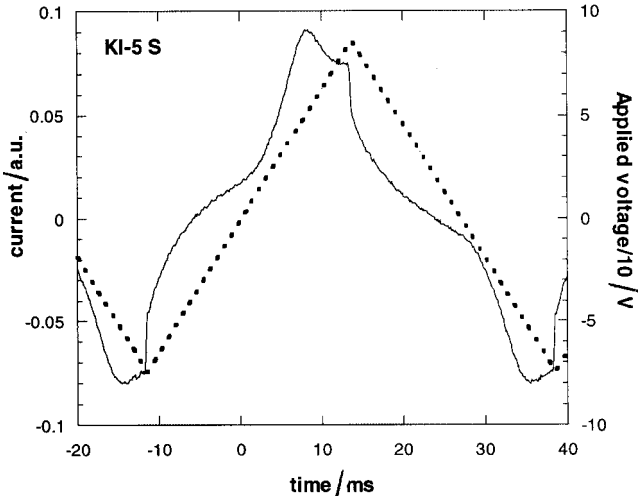

Figure 10. Switching current curves obtained by applying a triangular voltage wave: KI-5S (X = –C=C–) at 150°C ($\pm$ 20 V μm^{-1}, 20 Hz).

These two regimes originate from the modification of the equilibrium between cholesteryl/aromatic mesogen and cholesteryl/aliphatic tail interactions.

In the case of the current KI-5X compounds which possess the same cholesteryl moiety and the same aliphatic parts, several equilibrium states between the different driving forces can be observed depending on the nature of the linking group X of the aromatic mesogenic unit. Indeed, the cholesteryl/aromatic mesogen interactions will change since the distribution or repartition of the electrostatic potential along the molecules (drawn in blue in figure 12) is quite different from one KI-5X compound to another. According to this repartition, two groups of dimesogens can be distinguished:

(1) Molecules with a dissymetric potential lobe such as that in the benzoates dimesogens (–COO– and –OOC– groups). Note that the only difference between these two compounds lies in the reverse order of the ester groups i.e. –COO– vs. –OOC–. For the second of these, the very dissymetric and out of plane potential lobe disfavours the intermolecular lateral interactions and prevents the formation of a smectic phase.

(2) Molecules with a cylindrical symmetry of the negative potential with respect to the molecular long axis (X = –CH=CH–, –CH=N–, –N=N– and –C≡C–). For the Schiff's base (X = –CH=N–) and tolane (X = –C≡C–), the strong (and then

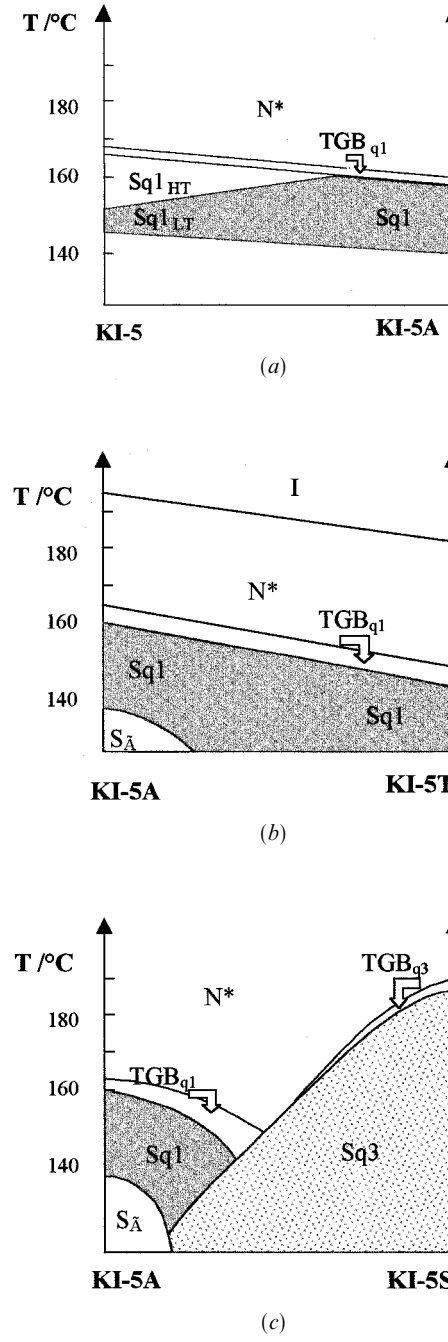

Figure 11. (*a*) Schematic drawing of a part of the KI-5/KI-5A binary phase diagram established from the study of binary mixtures [22]. (*b*) Schematic KI-5A/KI-5T binary phase diagram (contact method). The contact method provides the general shape of the phase diagram, but not a concentration scale. (*c*) Schematic KI-5A/KI-5S binary phase diagram (contact method).

Figure 9. Intensity profiles at low and wide angles (see insets) corresponding to the smectic phase of: (*a*) KI-5T (X = –C≡C–) at 140°C, (*b*) KI-5A (X = –N=N–) at 150°C, (*c*) KI-5 (X = –CH=N–) at 140°C (phases S_{q1LT}), (*d*) KI-5B (X = –COO–) at 140°C, (*e*) KI-5S (X = –C=C–) at 150°C, and (*f*) to the cholesteric phase of KI-5RB at 140°C.

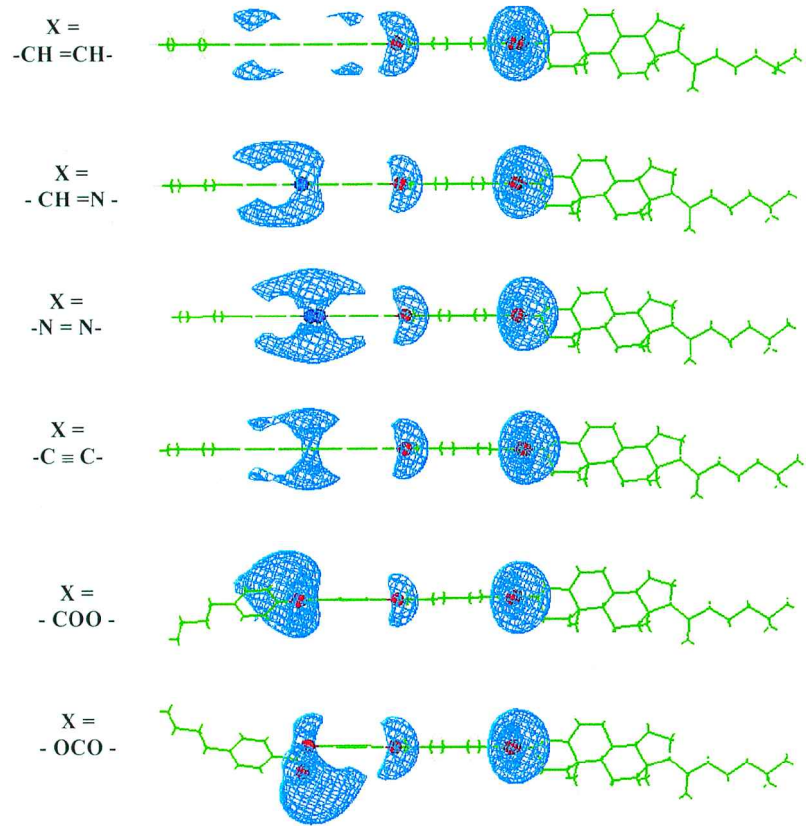

Figure 12. Representation of KI-5*X* dimesogens resulting from molecular dynamics and electrostatic potential calculations. Blue contours at $-40\,\mathrm{kJ\,mol^{-1}}$. Molecules are drawn in stick presentation with hydrogen omitted for clarity; O and N are represented as balls.

localized) negative potential is shifted onto the external aromatic ring, while for the azo compound ($X = -$N=N$-$) it remains centred on the linking group. In these three systems, the constraints due to electrostatic interactions between two adjacent dimesogens will be strong and highly influential and, as previously observed, this leads to the loss of the periodicity $q3$ connected with the cholesteryl length and to the development of the $q1$ periodicity. The stilbene dimesogen ($X = -$CH=CH$-$) is distinguished from the three others in this group by a very weak (and hence weakly localized) negative potential located only on the aromatic rings. In this last case, the electrostatic interactions become negligible, the overlapping of the cholesteryl moiety with the aromatic mesogen is greatly facilitated and as a result the $q3$ periodicity can develop.

This molecular analysis and the determination of favoured configurations of pairs of dimesogens does not describe the long range order in a smectic phase. Nevertheless, this approach underlines the differences in the local arrangement of the KI-5*X* compounds which may be responsible for the different characteristic lengths, and the conclusions are in agreement with the X-ray data.

As shown in table 3, the smectic parameter in the 'S_{q1} phases' remains significantly shorter than the molecular length: this suggests that the molecules which form the layered structure are either tilted molecules or bent. Molecular dynamics calculations, involving 80 KI-5 dimesogen molecules with periodic boundary conditions, clearly show as a result a bent conformation of the molecules in the case of different smectic arrangements (figure 13) [32]. In this sense the KI-5*X* non-symmetric dimesogens linked by a pentamethylene spacer can be compared to banana-shaped molecules, as recently observed for achiral dimesogens [33].

The difficulties encountered in this study in labelling the smectic phases using a classical nomenclature arise from the large variety of possible layer structures involving molecules with a bent shape, the chirality and helical structures, the different kinds of dimesogens and their overlapping, with, in addition, a cholesteryl mesogenic group which plays a specific role in the smectic layering. All these parameters can lead to a complicated

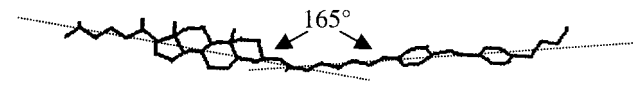

Figure 13. Conformation of one KI-5 molecule after molecular dynamics calculations including 80 dimesogen molecules.

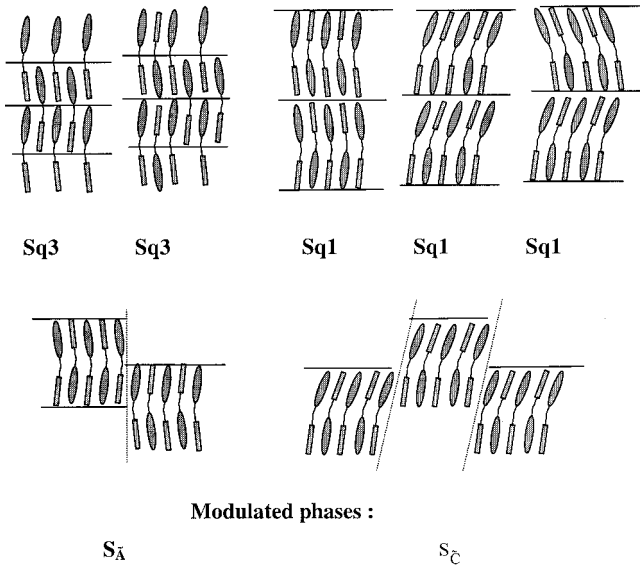

Figure 14. Schematic representations of some possible smectic packings.

polymorphism of tilted and/or non-tilted fluid smectic phases which cannot be described within the usual smectic nomenclature. Only some possibilities are imagined in figure 14.

Finally we note that the anomalies of periodicity represented by the simultaneous existence of two incommensurate wavevectors $q1$ and $q3$ are observed only for KI-5 (X = –CH=N–) and KI-5A (X = –N=N–). They potentially exist in the KI-5S compound (X = –CH=CH–) which exhibits a S_{q3} phase with '$q1$ fluctuations'. Indeed the periodicity connected with $q3$ is required to observe incommensurate phases or modulated phases. In conclusion, a general question is raised: how can an incommensurate layering arrangement exist or be induced in other dimesogenic systems? This point is currently under study using binary systems of two dimesogens, one showing a S_{q1} phase and the other a S_{q3} phase. In some peculiar cases, anomalies of periodicity are induced in the phase diagram through the occurrence of a genuine incommensurate smectic domain S_{ic}, but also at low temperature of an unexpected TGB-like phase, with a planar grey texture and incommensurate wave vectors. These results will be published in a forthcoming paper.

This collaborative research was cosponsored by the Science & Engineering Foundation of Korea and the CNRS of France.

References

[1] Hogan, J. L., Imrie, C. T., and Luckhurst, G. R., 1988, *Liq. Cryst.*, **3,** 645.
[2] Griffin, A. C., and Vaidya, S. R., 1988, *Liq. Cryst.*, **3,** 1275.
[3] Imrie, A. C., 1989, *Liq. Cryst.*, **6,** 391.
[4] Jin, J.-I., Kim, H.-S., Shin, J.-W., Chung, B. Y., and Jo, B.-W., 1990, *Bull. Korea chem. Soc.*, **11,** 209.
[5] Ikeda, T., Miyamoto, T., Kurihara, S., Tsukada, M., and Takuze, S., 1990, *Mol. Cryst. liq. Cryst.*, **182,** 357.
[6] Attard, G. S., Garnett, S., Hickmann, C. G., Imrie, C. G., and Taylor, L., 1990, *Liq. Cryst.*, **7,** 495.
[7] Jin, J.-I., Chung, B. Y., Choi, J.-K., and Jo, B.-W., 1991, *Bull. Korean chem. Soc.*, **12,** 189.
[8] Attard, G. S., Imrie, C. T., and Karasz, F. R., 1992, *Chem. Mater.*, **4,** 1246.
[9] Date, R. W., Imrie, C. T., Luckhurst, G. R., and Seddon, J. M., 1992, *Liq. Cryst.*, **12,** 203.
[10] Hardouin, F., Achard, M. F., Jin, J.-I., Shin, I.-W., and Yun, Y.-K., 1994, *Phys. II Fr.*, **4,** 627.
[11] Attard, G. S., Date, R. W., Imrie, C. T., Luckhurst, G. R., Roskilly, S., Seddon, J. M., and Taylor, L., 1994, *Liq. Cryst.*, **16,** 529.
[12] Marcellis, A. T. M., Koudijs, A., and Sudhölter, E. J. R., 1994, *Recl. Trv. Chim.*, **113,** 524.
[13] Hardouin, F., Achard, M. F., Jin, J.-I., and Yun, Y.-K., 1995, *J. Phys. II Fr.*, **5,** 927.
[14] Jin, J.-I., 1995, *Mol. Cryst. liq. Cryst.*, **267,** 249.
[15] Blatch, A. E., Fletcher, I. D., and Luckhurst, G. R., 1995, *Liq. Cryst.*, **6,** 18.
[16] Fletcher, I. D., and Luckhurst, G. R., 1995, *Liq. Cryst.*, **18,** 175.
[17] Date, R. W., Luckhurst, G. R., Shuman, M., and Seddon, J. M., 1995, *J. Phys. II Fr.*, **5,** 587.
[18] Marcellis, A. T. M., Koudijs, A., and Sudhölter, E. J. R., 1995, *Liq. Cryst.*, **18,** 843.
[19] Faye, V., Barois, P., Nguyen, H. T., Laux, V., and Isaert, N., 1996, *New J. Chem.*, **20,** 283.
[20] Faye, V., Babeau, A., Placin, F., Nguyen, H. T., Barois, P., Laux, V., and Isaert, N., 1996, *Liq. Cryst.*, **21,** 485.
[21] Faye, V., Nguyen, H. T., and Barois, P., 1997, *J. Phys. II Fr.*, **7,** 1245.
[22] Hardouin, F., Achard, M. F., Jin, J.-I., Yun, Y.-K., and Chung, S. J., 1998, *Eur. Phys. J.* **B1,** 47.
[23] Jin, J.-I., Kwon, Y.-W., Yun, Y.-S., Zin, W.-C., and Kang, Y.-S., 1998, *Mol. Cryst. liq. Cryst.*, **309,** 117.
[24] Le Masurier, P. J., and Luckhurst, G. R., 1988, *Liq. Cryst.*, **25,** 63.
[25] Hardouin, F., Achard, M. F., Laguerre, M., Jin, J.-I., and Ko, D.-H., 1999, *Liq. Cryst.*, **26,** 589.
[26] Grandjean, F., 1922, *C.r. Acad. Sci. Paris*, **172,** 71.
[27] Cano, R., 1968, *Bull. Soc. Fr. Min. Cryst.*, **91,** 20.
[28] Hardouin, F., Nguyen, H. T., Achard, M. F., and Levelut, A. M., 1982, *J. Phys. Lett.*, **43,** L-327.
[29] Sigaud, G., Hardouin, F., Achard, M. F., and Levelut, A. M., 1981, *J. Phys. Fr.*, **42,** 107.
[30] Demus, D., Demus, H., and Zasche, H., 1974, *Flüssige Kristalle in Tabellen* (Leipzig: VEB Deutscher Verlag für Grudstoffindustrie).
[31] Ribeiro, A. C., Dreyer, A., Oswald, L., Nicoud, J. F., Soldera, A., Guillon, D., and Galerne, Y. G., 1994, *J. Phys. II Fr.*, **4,** 407.
[32] Laguerre, M., unpublished results.
[33] Watanabe, J., Niori, T., Choi, S.-W., Takanishi, Y., and Takezoe, H., 1998, *Jpn. J. appl. Phys.*, **37,** L 401.